ChemElectroChem

Chemistry Europe
European Chemical Societies Publishing
ChemElectroChem

RESEARCH ARTICLE OPEN ACCESS

Exploration of Collagen as Binder for Aqueous Zinc Batteries and Symmetric Carbon Supercapacitors

Daria Mikhailova[1,2] | Evgenia Dmitrieva[1] | Mikhail V. Gorbunov[1,2] | Qiongqiong Lu[1,3] | Hoang Bao An Nguyen[1] | Ahmad Omar[1] | Niloofar Soltani[1] | Marit Baltzer[4] | Enno Klüver[2,4]

[1]Leibniz Institute for Solid State and Materials Research Dresden (IFW Dresden), Dresden, Germany | [2]Karlsruhe Institute of Technology (KIT), Institute for Applied Materials (IAM), Eggenstein-Leopoldshafen, Germany | [3]Institute of Materials, Henan Key Laboratory of Advanced Conductor Materials, Henan Academy of Sciences, Zhengzhou, P. R. China | [4]FILK Freiberg Institute gGmbH, Freiberg, Germany

Correspondence: Daria Mikhailova (daria.mikhailova@kit.edu) | Enno Klüver (enno.kluever@kit.edu)

Received: 23 February 2026 | **Revised:** 24 March 2026 | **Accepted:** 26 March 2026

Keywords: adjustable binder properties | biodegradable binder | biopolymers for battery application | electrochemically stable binder

ABSTRACT

Rechargeable water-based metal batteries attract great attention due to low cost, high safety merits, sustainable cell fabrication and an easier recyclability at the end of life. During cell design, the binder often remains without attention. In this study, aqueous dispersions of native collagen were successfully explored as binders in $Na_{0.44}MnO_2$, $Na_3V_2(PO_4)_3$, and V_2O_5-PEDOT cathodes for zinc batteries and in carbon electrodes for double-layer supercapacitors. The use of collagen is motivated by its environmental friendliness and high availability. Different functional groups in collagen are capable to chelate metal cations and are viable for chemical cross-linking. Collagen shows high water binding capacity, reasonable thermostability, a wide electrochemical stability window between −1.0 and 1.2 V versus Ag/AgCl and water-based processability of electrodes. Intrinsic properties of collagen dispersions like viscosity or pH value can be easily adapted. The pH value of the dispersion has a noticeable impact on the reaction mechanism in electrodes: cycling behavior of V_2O_5-PEDOT cathodes with acidic collagen dispersion providing 335 mAh g^{-1} capacity in the 300th cycle, is much more stable than that of cathodes with neutral collagen dispersion or CMC binder due to suppression of PEDOT oxidation, which occurs in the neutral medium at the end of charge.

1 | Introduction

Besides the active components of a metal-ion battery such as electrodes and electrolyte solutions, the binder also plays an important role, which is often underestimated. The task of the binder implies creating a coherent contact between the particles of the active electrode material and conductive additive with each other and the current collector. As a dispersing and thickening agent, the binder ensures homogeneous distribution of the components and provides mechanical stability. It maintains the electric contact for electron movement and facilitates ionic transport in the electrode through increased wettability. A multitude of parameters are relevant for the use of a binder like chemical, electrochemical, thermal, and mechanical stability; stability against solvent; electronic and ionic conductivity; rheology; and adhesion [1]. The binder should not undergo chemical reactions with cathode, anode and electrolyte under operating conditions. It should be stable over a wide range of voltages during battery charging and discharging, especially it should not be reduced at low negative potential and not oxidized at high positive potential. Temperature change plays a role in battery production (when drying dissolved binders) and operation at elevated temperatures. The typical operating range of batteries lies between −20°C and 55°C [2]. Temperature changes can also cause expansions of the binder and affect diffusion. The binder should not dissolve in the used electrolyte. The usually low electronic conductivity of polymers can be increased by doping with suitable additives (π-electron systems, oxidative or reductive groups) or by adding conductive additives. Ionic conductivity

is conditioned by the crystallinity grade, porosity, and viscosity of the polymer. In general, polymers containing many functional groups that can form strong hydrogen bonds (e.g., cellulose or polyacrylic acid) show a sufficient adhesion to the current collector and electrode materials. As the volume of the electrodes may change during operation, and mechanical stress (bending) is possible in the case of portable batteries, adhesion plays a major role in maintaining integrity. The viscosity of the dissolved or dispersed binder is important when used for electrode assembly, since the binder must penetrate well into the porous material. This process also depends on the structure of the electrodes themselves and can be influenced by adding dispersing additives. Hard binders generally show better adhesion and stability during cycling. Elasticity is necessary for compensating volume expansion of electrodes and can be reasonable in developing batteries for portable devices.

Despite its low mass fraction of 2%–8%, the binder contributes significantly to the electrochemical performance of the metal-ion battery. Currently, polyvinylidene fluoride (PVDF) is commonly used for batteries with organic and aqueous electrolyte solutions due to its polymer structure and its mechanical, chemical, and electrochemical stability [1]. However, due to the high fluorine content and the need for toxic N-methyl-2-pyrrolidone as a solvent, the use of PVDF is unfavorable from the ecological and safety point of view. In addition, recycling of electrode materials with the PVDF binder could be complicated.

Biopolymers are a promising sustainable alternative for binders in electrochemical applications in order to avoid synthetic polymers like PVDF. Recent investigations focused on carbohydrates, mainly carboxymethyl cellulose (CMC) and sodium alginate, but also studies on chitosan, xanthan, starch, agar–agar, etc. are reported (see [1, 3, 4] and references therein). These carbohydrate binders were combined with different electrode types in lithium- as well as sodium-ion batteries. The performance of electrochemical cells with the CMC binder is comparable with the established PVDF binder in many aspects like adhesion, discharge capacity, and capacity retention, while the swelling in organic electrolytes is even lower [5–11]. Proteins as another large biopolymer class are rarely investigated as electrochemical binders. There is only a small number of reports on gelatin in combination with graphite anodes in lithium-ion batteries [1, 4, 12–15]. The gelatin binder is electrochemically stable and comparable with PVDF in terms of enabling respective electrode specific capacity and capacity retention. However, gelatin has inferior rheological properties, showing partially shear thinning and partially shear thickening behavior, which is unfavorable for electrode coating. Moreover, gelatin is thermally stable only below 30°C and highly soluble in aqueous medium at elevated temperatures. Since gelatin is a degraded derivative of collagen, a potential alternative is the use of native collagen dispersions. These dispersions comprise an aqueous suspension of shredded collagen fibers, which form a natural network of protein chains with high water-binding capacity and a variety of ionizable functional groups. Their advantage over gelatin is a polymer network with a higher molecular weight, constant shear thinning behavior, low solubility, and a higher thermal stability. The viscosity of native collagen dispersions can be easily adjusted by dry mass content, pH value, salt content, temperature, and cross-linking degree [16–19].

Collagen is the most common structural protein of animals and comprises about 30% of the total protein content. It is the main constituent of the extracellular matrix of connective tissues, such as skin, tendon, cartilage, ligament, and bone. Nowadays, 28 types of collagens are known with type I being the most abundant and most important [20–22]. The basic structural unit of collagen type I is a heterotrimer consisting of three helical protein chains (α-chains), which are twisted around each other to form a triple helix. These rod-like molecules are ordered in parallel in a staggered manner and form fibrils and fibers (Figure 1). On a higher hierarchical level, fibers are arranged into fiber bundles and fiber networks, which are the structural basis of form and shape for various tissues and organs [23–25]. The thermal and mechanical stability of collagen strongly depends on the intermolecular cross-linking of collagen proteins. Natural cross-links are generated in the organism enzymatically and connect the side chains of the amino acids lysine and hydroxylysine. In the manufacturing of collagen-based products, synthetic cross-links are often introduced to enhance the stability [26–30]. Covalent cross-links between amino acid side chains are formed using divalent reagents, like glutardialdehyde or carbodiimides [31–35]. Trivalent metal cations have the ability to form non-covalent cross-links by electrostatic and complex interactions, which is the chemical basis for leather tanning with chromium, aluminum or iron salts [36, 37]. Collagen as a biopolymer is the material basis for a number of products in different application fields like clothing (leather), food (sausage casings, gelatin, dietary supplement), packaging (coatings, adhesives), pharmaceutics (drug carrier, capsules), and medicine (wound dressing, implant material, suture material, tissue engineering) [38–42]. The manufacturing technologies for these products make use of collagen at different stages of processing and degradation, from the intact fibrous collagen matrix to highly degraded gelatin or protein hydrolysate [29].

The focus of the present work lies essentially on the principal suitability of native collagen as binder in water-based electrochemical energy storage systems. Aqueous Zn batteries with transition metal oxide electrodes and aqueous double-layer supercapacitors with carbon electrodes were chosen for

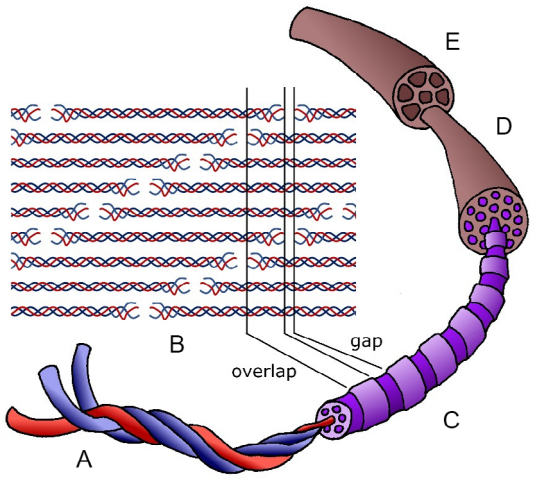

FIGURE 1 | Schematic view of the hierarchical collagen structure. (A) Triple helix of collagen α-chains $[\alpha1]_2[\alpha2]$. (B) Staggered alignment of triple helices leads to regions with less (gap) and more (overlap) density, resulting in the characteristic periodic striation of collagen fibrils. (C) Fibril. (D) Fiber. (E) Fiber bundle.

validation based on their well-known characteristics and satisfactory cyclability. In parallel to collagen, commercial PVDF and CMC were tested in electrochemical cells mostly under the same conditions.

In combination with other relatively harmless components of the battery cell (zinc-based aqueous electrolytes, Zn anode), an efficient aqueous battery with collagen binder was developed without toxicological or ecological issues, thus presenting a significant improvement in production, application and recycling compared to current lithium-ion technology.

2 | Experimental

2.1 | Declaration of Approval for the Use of Animal-Derived Materials

Food grade porcine skins were purchased from a local slaughterhouse. The material was processed at FILK Freiberg Institute with approval and under supervision of the Office for Veterinary Affairs and Food Safety.

2.2 | Collagen Preparation and Modification

Porcine skin was completely dehaired by alkaline treatment with calcium hydroxide according to common liming processes as established in leather production (pH 12.5, 72 h). After neutralization and deliming, the hairless pelt was comminuted in several subsequent steps into a homogeneous dispersion. In a first step, the skin was crushed in a mincer through several perforated disks down to a particle size of approximately 1 mm. The resulting granulate was swollen in acid solution at pH 2.8–3 overnight and then further comminuted in a magic PLANT device (IKA GmbH, Staufen, Germany), which presses the material through slits with a rotor/stator technique. By pumping the material several times (2–6) through the magic PLANT, increasing grades of grinding with decreasing fiber size were obtained. The pH value was constantly controlled and kept at 2.8 by addition of acid, when necessary. Final dispersions were neutralized and freeze-dried, which increased the dry mass content by water removal. For application and rheological measurements, the concentrated material was resuspended in acid solution (pH 3) with a defined dry mass content. Usually, acetic acid was used throughout. In additional experiments, hydrochloric acid and citric acid were used instead. Dispersion parameters, which were adjusted during the described preparation process, are dry mass content, acid type, and grinding grade. Covalent cross-linking of as prepared collagen dispersions was achieved by addition of glutaraldehyde (25% solution, synthesis grade, Sigma–Aldrich). Small volumes of 25% glutaraldehyde (0.04, 0.064 and 0.2 ml) were mixed with 50 ml water and added to 50 ml of a 2% collagen dispersion under vigorous stirring, resulting in 1% collagen dispersions with 1%, 1.6%, and 5% glutaraldehyde. $Fe_2(SO_4)_3$ (puriss. p. a., Honeywell/Fluka) was added to dispersions in varying amounts for noncovalent cross-linking via chelating effects. $Fe_2(SO_4)_3$ (50, 100 and 200 mg) was added to 100 ml of a 1% collagen dispersion under vigorous stirring, resulting in dispersions with 5%, 10%, and 20% Fe(III) sulfate.

2.3 | Collagen Characterization

2.3.1 | Moisture Content

A collagen sample was weighed before and after drying (102°C, 5 h). The moisture content (%) was calculated from the mass difference in relation to the initial sample weight. The dry mass content (d.m.) is 100 %− moisture content.

2.3.2 | Ash Content

A collagen sample (0.5–2 g) was annealed in a platinum crucible for 2 h at 600°C in a muffle furnace. After cooling down in a desiccator, the residue was weighed. The ash content was calculated in relation to the dry mass content (% d.m.).

2.3.3 | pH Value

A collagen sample (ca. 5 g) was agitated in 100 ml distilled water for 6 h at 20°C. The supernatant was decanted and the pH was measured using a glass electrode.

2.3.4 | Amino Acid Profile

A collagen sample (ca. 1.5 mg) was treated with 1.5 ml 6 N HCl for 20 h and then dried, and the residue was dissolved in lithium citrate buffer (pH 2.2). 30 µl of the resulting amino acid solution were injected into an amino acid analyzer Biochrom 30 plus (Onken, Gründau, Germany), where the amino acids were separated chromatographically, derivatized with ninhydrin and detected at wavelengths 440 and 570 nm. The concentration of each amino acid was calculated from the corresponding peak areas, according to calibration with an amino acid standard. The method does not allow the distinction between asparagine (Asn) and aspartic acid (Asp) or glutamine (Gln) and glutamic acid (Glu), and tryptophan (Trp) is not detected. The amount of lysine (Lys)/hydroxylysine (Hyl) is a measure for the cross-linking degree after introduction of covalent cross-links by glutaraldehyde. Decreasing lysine/hydroxylysine content indicates increasing cross-linking. These values are only relevant for acid-stable cross-links in glutaraldehyde-treated samples. In all other materials, the amino acid profile remains unaltered. Therefore, amino acid analysis was not performed for all dispersions.

2.3.5 | Differential Scanning Calorimetry (DSC) Measurements

A collagen sample was soaked in phosphate buffer (pH 7) for 2–5 h. DSC measurement was performed in a differential scanning calorimeter "DSC7" (Perkin Elmer, Waltham, USA) using an aluminum crucible in a temperature interval from 15°C to 100°C with a heating rate of 5°C/min. Onsets and maxima of peaks were determined from the graphical display of heat flow versus temperature.

2.3.6 | Surface Energy of Collagen Films

Collagen films were prepared from selected collagen dispersions (acidified with acetic acid or hydrochloric acid, modified with glutaraldehyde or iron(III) sulfate and with different grinding grade). Collagen dispersions (60 g) were cast into laboratory dishes and dried at 25°C in air for 16 h. The surface energy of the resulting collagen films was determined by contact

angle measurements with three liquids of different polarity: water, ethylene glycol, and diiodomethane (measurement system OCA35, DataPhysics Instruments, Germany). The surface energy (total, polar, and dispersive components) was calculated according to the OWRK method (Owens, Wendt, Rabel, and Kaelble model) as provided with the device's software SCA20 U. The polarity is defined as the ratio of polar component to total surface energy.

2.3.7 | Rheology

A sample of collagen dispersion was placed between the plates of an MCR 502 rheometer (Anton Paar, Ostfildern, Germany). Measuring parameters were: plate/plate geometry (diameter 25 mm, slit width 1 mm), and 25°C. The dispersion was measured at 6 different shear rates (10, 20, 40, 60, 80 and 100 s^{-1}) and the viscosity was recorded. Rheological characteristics are displayed in Figure 2 in a double logarithmic graphical representation of viscosity versus shear rate. The shear viscosity decreases with increasing shear rate, according to the power law model $\eta = k^*\gamma^n$ for non-Newtonian fluids.

2.4 | Electrochemical Stability of Collagen Suspensions

The electrochemical stability windows of aqueous collagen suspensions were determined by cyclic voltammetry measurements at room temperature using three-electrode cells with a glassy carbon (GC) working electrode, platinum mesh counter electrode, and a standard aqueous Ag/AgCl reference electrode (3M NaCl, $E = 0.195$ V vs. RHE). The experiments were done on a HEKA potentiostat/galvanostat (HEKA Elektronik GmbH, Germany) with a scan rate of 50 mV/s. Aqueous collagen suspensions without adding any salts were used as electrolytes. The measurements were done under Ar-atmosphere (with an O_2 content less than 0.1%).

2.5 | Preparation of Working Electrodes with Collagen for Zn Batteries and Symmetric Supercapacitors

2.5.1 | Carbon Black (CB)

As electrode material, Carbon Black Super C65 (Imerys Graphite & Carbon) was weighed with collagen in a mass ratio of 7:3 (based on the collagen dry mass) and thoroughly mixed. The mixture was then carefully spread between two carbon foils with diameter of 10 mm and evenly distributed in order to form the electrode for the aqueous battery. A typical active mass for carbon electrodes was around 2.5–3.0 mg.

2.5.2 | Commercial YP50F Carbon

Carbon electrodes were prepared using a mixture of 95% YP50F carbon (Kuraray Chemical. Co., Japan) and 5% (w/w) collagen dispersion with pH = 3 (based on the collagen dry mass), and water as solvent for slurry preparation, which was well-mixed in a Retsch MM200 shaker mill using steel balls at 25 Hz for 30 min. Then, the slurry solution was coated on graphite foil current collector using doctor blade coating method and dried in air under ambient conditions. Electrodes of 10 mm diameter were used for the tests (mass loading between 2 and 3 mg per electrode).

2.5.3 | Poly(3,4-Ethylenedioxythiophene)-Coated V_2O_5 (V_2O_5-PEDOT)

7 g of commercial V_2O_5 powder (Sigma–Aldrich) were dispersed in 70 mL of deionized water by stirring. After that, 3 mL of 3,4-ethylenedioxythiophene (EDOT, Aladdin) were added dropwise. The mixture was continuously stirred for 6 days, during this process, the color of the mixture changed from yellow to green. The obtained composite was dried overnight in a vacuum oven at 70°C for further use. The phase purity was confirmed by X-ray powder diffraction (XRD) using a STOE STADI P diffractometer with Co Kα1 radiation, equipped with a Mythen 1K detector, in

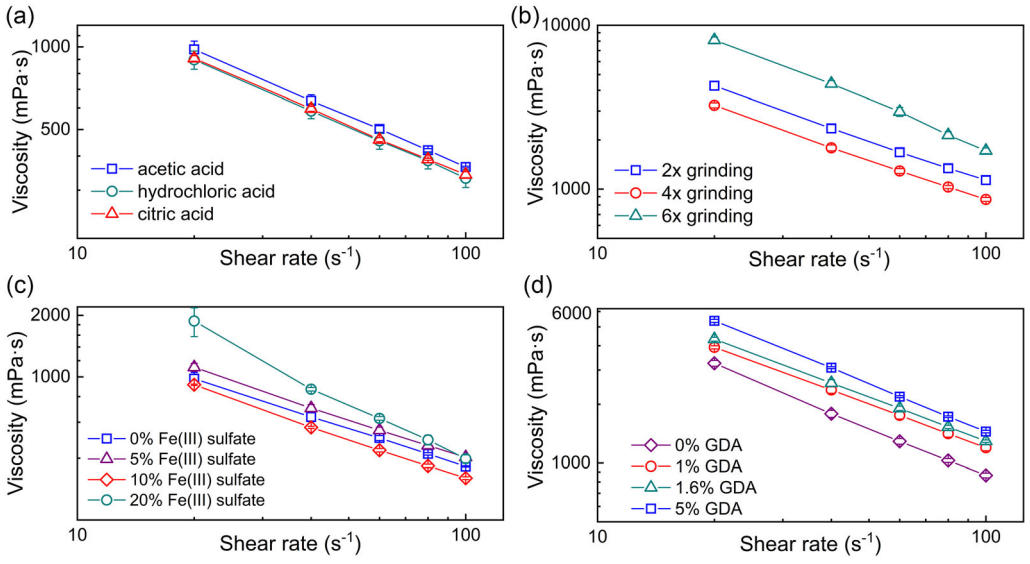

FIGURE 2 | Rheological characterization of modified collagen dispersions showing the influence on the viscosity for (a) acid type, (b) grinding grade, (c) Fe(III) salt, and (d) covalent cross-linking content. Average values from triplicates, standard deviations are included.

transmission mode. Fourier transform infrared (FTIR) spectroscopy studies were carried out using a PerkinElmer FTIR spectrometer.

The V_2O_5-PEDOT electrodes were prepared by coating the slurry of active material, Super C65 (TIMCAL, Switzerland), and binder in water at a mass ratio of 7:2:1 onto a stainless-steel mesh and then dried at 70°C overnight. The mass loading of the active material was approximately 2.5 mg cm^{-2}.

As a comparison, the coated V_2O_5-PEDOT electrode was prepared with the same mass ratio using carboxymethyl cellulose (CMC) binder.

2.5.4 | $Na_{0.44}MnO_2$ (NMO) and $Na_3V_2(PO_4)_3$ (NVP)

$Na_{0.44}MnO_2$ was synthesized via a solid-state route from Na_2CO_3 (Sigma Aldrich, 99.9%), taken with a 7% molar excess, and Mn_2O_3 (Alfa Aesar, 99.9%). Both chemicals were ground in an agate mortar, pressed into a pellet, and annealed in air at 600°C for 20 h, with one intermediate grinding. The phase purity was confirmed by XRD method using a STOE STADI P diffractometer with Co Kα1 radiation, equipped with a Mythen 1K detector, in transmission mode.

For electrode preparation, NMO and purchased NVP (MSE Supplies, USA) were mixed with CB and a collagen binder with the mass ratio of 8:1:1, considering the collagen dry mass. Electrode sheets of respective materials were prepared using the doctor-blade technique. In each case well-mixed aqueous slurry with CB and binder was prepared using a Retsch MM200 shaker mill. Mixing was done with steel balls at 25 Hz for 30 min. Coating was performed using a blade with 300 µm blade height at 2.5 mm/s translation under ambient conditions with subsequent drying of the materials in air. As substrates for coating, graphite foil or carbon paper were used.

For comparison, a coated NVP electrode was fabricated using polyvinylidene fluoride (PVDF) binder with the same mass ratio.

2.6 | Cell Assembly and Electrochemical Tests of Zn Batteries and Symmetric Supercapacitors

Zinc foil (50 µm thickness) was punched into circular pieces with a diameter of 12 mm as the counter electrode. Before use, the surface of the zinc foil was fully polished with sandpaper, rinsed thoroughly with distilled water, and dried. The electrodes were then inserted into a Swagelok cell or CR2025 coin cells and assembled into a complete battery cell using a glass-fiber separator (Whatman GF/D) with a diameter of 12 mm, and a 3 M zinc trifluoromethanesulfonate (zinc triflate, $Zn(SO_3CF_3)_2$, purity ≥98%, Sigma–Aldrich) solution as electrolyte. For Swagelok cells, 250 µl of electrolyte was used, while 200 µl for coin cells.

Electrochemical tests were performed in two-electrode set-up always two or three times for each experiment for reproducibility confirmation. In case of carbon-based supercapacitors and V_2O_5-PEDOT and $Na_{0.44}MnO_2$ cathode materials, the capacity values represent the average of two or three cells, while in case of $Na_3V_2(PO_4)_3$ materials in Zn batteries with change of the reaction mechanism upon cycling, the most typical cell behavior is shown as results.

Cyclic voltammetry (CV) measurements of symmetric carbon supercapacitors with almost identical electrode masses were performed on a VMP3 (Biologic, France) potentiostat in the voltage range $\Delta V = 0.8$V. As electrolytes, 1 M aqueous solutions of Zn triflate, Na triflate, and Na_2SO_4 were tested. For measurements, Swagelok-type cells with a two-electrode configuration were used. The scan rates ν ranged from 2 to 500 mV s^{-1}. Calculations of the discharge capacitance of the two-electrode cell (C_{cell}) and of each electrode ($C_{electrode}$), which are connected in series, were performed using the formula $C_{electrode} = 2{*}C_{cell}$. Specific capacitance of the electrode C_{sp} was calculated using the electrode mass m and the total intergared area:

$$C_{sp} = \frac{\int I(V)dV}{\nu m \Delta V}$$

Galvanostatic cycling with potential limitation (GCPL) was performed on Battery Test System (BaSyTec GmbH, Germany) and VMP3 (Biologic, France) potentiostats. In this case, specific discharge capacitance of the electrode C_{sp} in symmetric supercapacitors was calculated as:

$$C_{sp} = \frac{2I\Delta t}{m\Delta V}$$

All measurements were conducted at 25°C using temperature-controlled climate chambers. Specific capacity was calculated based on the mass of the active material in each electrode. Multiple cells were tested under the same conditions to ensure reproducibility.

3 | Results and Discussion

3.1 | Physicochemical Characterization of Native and Modified Collagens

A standard collagen dispersion with pH 3 was prepared using acetic acid and fourfold grinding without other additives. Modified dispersions were produced with varying acid type, pH value, dry mass content, grinding grade and addition of Fe(III) salt and glutaraldehyde. The influence of the modifications on the thermal stability (as shown by the denaturation temperature), cross-linking degree, and rheological properties were analyzed. The data are shown in Table 1.

3.1.1 | Dry Mass Content and pH Value

In terms of practical handling, a collagen dispersion with 1% dry mass content and pH 3 is favorable. A higher dry mass content increased the viscosity (data not shown) and the thermal stability (Table 1). A collagen dispersion at neutral pH tends to segregate due to the proximity to the isoelectric point. Thus, the preparation of a homogeneous neutral collagen dispersion requires increased mechanical effort.

3.1.2 | Acid Type

Acetic acid is used by default in the preparation of acidic collagen dispersions. Since acetic acid is prone to redox processes, its presence may have an influence on the electrochemical performance of collagen. Therefore, alternative acids, hydrochloric acid and citric acid, were also used. No significant influence of the acid type on thermal stability or viscosity was detected (Table 1, Figure 2).

TABLE 1 | Characteristic parameters of collagen dispersions. The abbreviations have following meanings: d. m., dry mass content; T_D, denaturation temperature; GDA, glutaraldehyde; Lys, lysine; Hyl, hydroxylysine; n.d., not determined.

No.	d.m., %	Acid	Grinding grade	Additive	pH	Ash, % d.m.	T_D, °C	Sum Lys+Hyl, Mol-%
1	1.0	Acetic	4x	—	3.0	0.07	43.46	3.40
2	1.0	Acetic	4x	—	7.0	0.14	51.85	3.42
3	2.0	Acetic	4x	—	3.0	0.25	41.20	3.40
4	2.0	Acetic	4x	—	7.0	0.23	54.32	3.42
5	1.2	Acetic	4x	—	3.1	0.04	40.28	n.d.
6	1.2	HCl	4x	—	3.0	0.04	40.61	n.d.
7	1.3	Citric	4x	—	3.0	0.03	41.18	n.d.
8	1.3	Acetic	4x	5% $Fe_2(SO_4)_3$	3.0	0.07	40.67	n.d.
9	1.4	Acetic	4x	10% $Fe_2(SO_4)_3$	2.8	0.10	42.45	n.d.
10	1.4	Acetic	4x	20% $Fe_2(SO_4)_3$	2.5	0.18	41.07	n.d.
11	1.3	Acetic	2x	—	3.0	0.00	41.28	n.d.
12	1.1	Acetic	4x	—	3.1	0.01	41.53	n.d.
13	1.1	Acetic	6x	—	3.1	0.00	41.71	n.d.
14	1.0	Acetic	4x	1% GDA	3.0	0.50	43.46	2.94
15	1.0	Acetic	4x	1.6% GDA	3.1	0.50	43.54	3.17
16	1.1	Acetic	4x	5% GDA	3.0	0,40	42.96	1.98

3.1.3 | Grinding Grade

Fourfold grinding in the magic PLANT is an established standard procedure for preparing a homogeneous collagen dispersion. Although it is not possible to correlate the number of grinding steps with a certain fiber size, the grinding grade serves as a describing parameter. Two dispersions were prepared with less (2x) and more (6x) grinding steps, corresponding to larger and smaller fibers. While there was no influence on the thermal stability, the viscosity of the dispersions increased in both cases, for increased and reduced grinding (Figure 2). This may be attributed to two opposite effects. On one hand, increased grinding reduces the entanglement of collagen fibers which leads to a decrease in viscosity [43]. On the other hand, increased grinding creates a higher fiber surface area, thus probably enhancing the number of attractive forces between the fibers, which increases the viscosity [19]. Thus, a viscosity minimum with reduced fiber entanglement and medium surface interactions is observed for fourfold grinding.

3.1.4 | Fe(III) Salt

Fe(III) sulfate was added in increasing amounts. It is known that iron ions have some chelating effect with carboxylic and amino groups of collagen side chains [44, 45], which is the basis for iron tanning activity in leather production [37]. It was expected that this effect may influence the viscosity or homogeneity. On the other hand, Fe^{3+}/Fe^{2+} is a redox-active ion pair which may influence the electrochemical performance. Depending on the amount of Fe(III) salt, the ash content slightly increased (Table 1). Any significant influence on the thermal stability was not detected. The viscosity increased with increasing Fe(III) sulfate concentration, which indicates chelating interactions between Fe^{3+} and collagen side chains.

3.1.5 | Glutaraldehyde

Bifunctional glutaraldehyde was added in order to introduce synthetic cross-links into the collagen material, which is a widely established procedure in the production of collagen-based products [26, 29, 31, 35]. An influence on the thermal stability was detected, as shown by the increasing denaturation temperature (Table 1). The decreasing lysine/hydroxylysine content indicates an increasing cross-linking degree of collagen, as expected. However, the high kinetics of the reaction may cause local differences and inhomogeneities, resulting in nonsystematic deviations of the measured values. The viscosity increased with increasing glutaraldehyde concentration and cross-linking degree (Figure 2). Glutaraldehyde was chosen as a model cross-linker, which is widely established and well known. Although glutaraldehyde itself is considered toxic, it should be stated that it is harmful only as a pure and highly reactive substance. After the cross-linking reaction, the collagen material contains non-reactive carbohydrate linkers, which do not cause toxicity. Residual glutaraldehyde is carefully washed out. Thus, glutaraldehyde is still used as a cross-linker even in medical products. However, there are less harmful alternatives for cross-linking which may be considered for a future industrial implementation. These include carbodiimides, diisocyanates, enyzmes, or plant-based aldehyde derivatives.

3.1.6 | Surface Energy of Collagen Films

Independent on the type of modification of the collagen dispersions and despite the hydrophilic nature of collagen, air-dried

collagen films showed a rather hydrophobic behavior. The water contact angles were above 90° throughout, while the calculated surface energies ranged from 30.4 to 46.1 mN/m with polarities below 5% (data not shown). While the influence of glutaraldehyde cross-linking was not distinct, addition of iron(III) salt and an increased grinding grade tended to increase the surface energy. It is likely that these findings can be ascribed to surface effects rather than to intrinsic material properties. It is known that air-drying of collagen dispersions generates a more closed surface in contrast to freeze-drying, which results in a porous structure [46, 47]. A compact surface may appear more hydrophobic than the underlying bulk material. On the other hand, literature data describe that the electrochemical performance of a battery depends on the compatibility of the components. Thus, a high affinity of the binder to carbon black as conductive additive enables a more homogeneous particle distribution and better performance [48]. The surface energy of carbon black is reported as 31.7 mN/m with a polarity below 10%, suggesting a good affinity to collagen [48].

3.2 | Electrochemical Stability Window of Collagen Dispersions

In first experiments, a glassy carbon (GC) electrode was coated by collagen from collagen dispersions with pH3 and pH7 and tested in degassed 1 M Na_2SO_4 electrolyte solution against a Pt counter electrode. Electrochemical cells with uncoated GC electrodes were used as a reference (Figure S1a). In the cells with uncoated GC, oxygen and hydrogen evolution occur at 1.2 V and −1.5 V versus Ag/AgCl, respectively, whereas these processes are almost suppressed in the cells with collagen-coated GC electrodes. Thus, the collagen film is less penetrable for water molecules, serving as a protection layer on the electrolyte surface, and no information about its electrochemical stability could be obtained in this set-up.

Therefore, we used aqueous collagen dispersions in the cell as "electrolytes" for estimation of their electrochemical stability. The impact of the acid, which was added for keeping the pH value of the collagen dispersion at 3, was studied first (Figure 3a). All cells show a nearly stable electrochemical window between −1.0 and 1.2 V versus Ag/AgCl reference electrode being positively and negatively charged with 50 mV s^{-1} scan rate. Below −1.0 V, irreversible H_2 evolution was observed, while O_2 evolution took place above approximately 1.3 V. The intensity of the gas evolution is directly proportional to the measured current value, which is similar for citric and acetic acid and slightly lower for HCl during reduction. The observed current at the positive potential during oxidation is significantly lower in case of acetic acid. Therefore, further experiments were carried out using collagen dispersions with acetic acid, since stable cycling of the aqueous battery cell with collagen is limited by the reaction at the cathode side. The electrochemical stability window of collagen slightly narrows with increasing cycling number for all studied acids.

Adding Fe(III) ions to the collagen dispersion impacts its electrochemical activity. On the one hand, Fe(III) can be coordinated by oxygen from -COOH and -CO groups and by nitrogen from -NH_2 groups of amino acids [44, 45]. This chelating effect to collagen is exploited in iron(III) based tanning processes [37]. On the other hand, Fe(III) cations are redox-active ($Fe^{3+} \leftrightarrow Fe^{2+}$) in the studied potential window. The Fe-modified collagen dispersions showed enhanced activity at low potentials (H_2 formation), which increases with the Fe concentration (Figure 3b). Very likely, Fe^{3+} ions act as a catalyst for water reduction, in accordance with the literature [49]. A narrowed potential range (limited to −1.4 V vs. Ag/AgCl) suppressed hydrogen evolution and revealed a reversible $Fe^{3+} \leftrightarrow Fe^{2+}$ redox process. As anticipated, the current intensity increases with the increasing concentration of the Fe ions in collagen dispersions. The difference between oxidation and reduction peak potentials is rather large, showing Fe^{2+} oxidation at 1.0 V and Fe^{3+} reduction at −0.25 V for the collagen dispersion with 20% $Fe_2(SO_4)_3$.

As reference systems, we determined oxidation/reduction potentials of Fe in an aqueous $FeSO_4$ solution (stabilized with H_2SO_4 against hydrolysis), $Na_4[Fe(CN)]_6$ solutions (with addition of Na_2SO_4 electrolyte salt), and in ferrocene, dissolved in acetonitrile (Figure S1b). In the $FeSO_4$ solution with Fe cations surrounded by water molecules in the first coordination sphere, Fe oxidation was observed at 0.55 V, while reduction occurred at 0.35 V (vs. Ag/AgCl). Since the collagen dispersion was modified by addition of $Fe_2(SO_4)_3$ solutions of different concentrations, oxidation/reduction peaks of Fe could be expected at similar potentials supposing no chelating effect between Fe^{3+} and collagen occurs. In our case, a noticeable difference between redox processes in $FeSO_4$ and Fe modified collagen dispersion certainly points to a complexation of Fe^{3+} by collagen, which can be interpreted as chelate-based cross-linking process.

A covalent type of cross-linking was created by the reaction between -NH_2 groups of lysine and hydroxylysine and glutardialdehyde, which leads to the formation of a Schiff base of general formula R-N=CH-R'. This type of cross-linking notably weakens the stability of collagen at high potentials (Figure 3c), which also decreases with the number of cycles. Mechanical treatment of the collagen dispersion via repeated grinding also impacts its electrochemical stability: Fourfold grinding seems to warrant a stable long-term behavior; otherwise, time-dependent instability was observed in cyclic voltammetry measurements (Figure 3d). Since repeated grinding affects the size of collagen fibers in the dispersion, there seems to be an optimal fiber size for electrochemical applications. Unfortunately, the fiber size (length, diameter) is analytically not accessible and cannot be expressed in concrete values.

A neutral collagen dispersion (pH = 7) shows the onset of oxygen oxidation already at 1.1 V vs. Ag/AgCl (Figure S2), but is more stable against hydrogen reduction, demonstrating at −1.5 V the lowest current in comparison to dispersions with pH = 3.

3.3 | Electrochemical Behavior of Collagens in Aqueous Zn Batteries

The electrochemical stability of collagen in Zn batteries was proven with a mixture of collagen and carbon black as working electrode in a 3 M Zn triflate electrolyte solution (Figure 4), using CV measurements with 0.1 mV s^{-1} scan rate. Here, the impact of acids used for the preparation of acidic collagen dispersions with pH = 3 was elaborated as well for the stable window of the battery. Thus, among collagen dispersions with acetic acid, hydrochloric acid and citric acid, the dispersion with acetic acid shows the lowest stability below 0.2 V versus Zn^{2+}/Zn, followed by citric

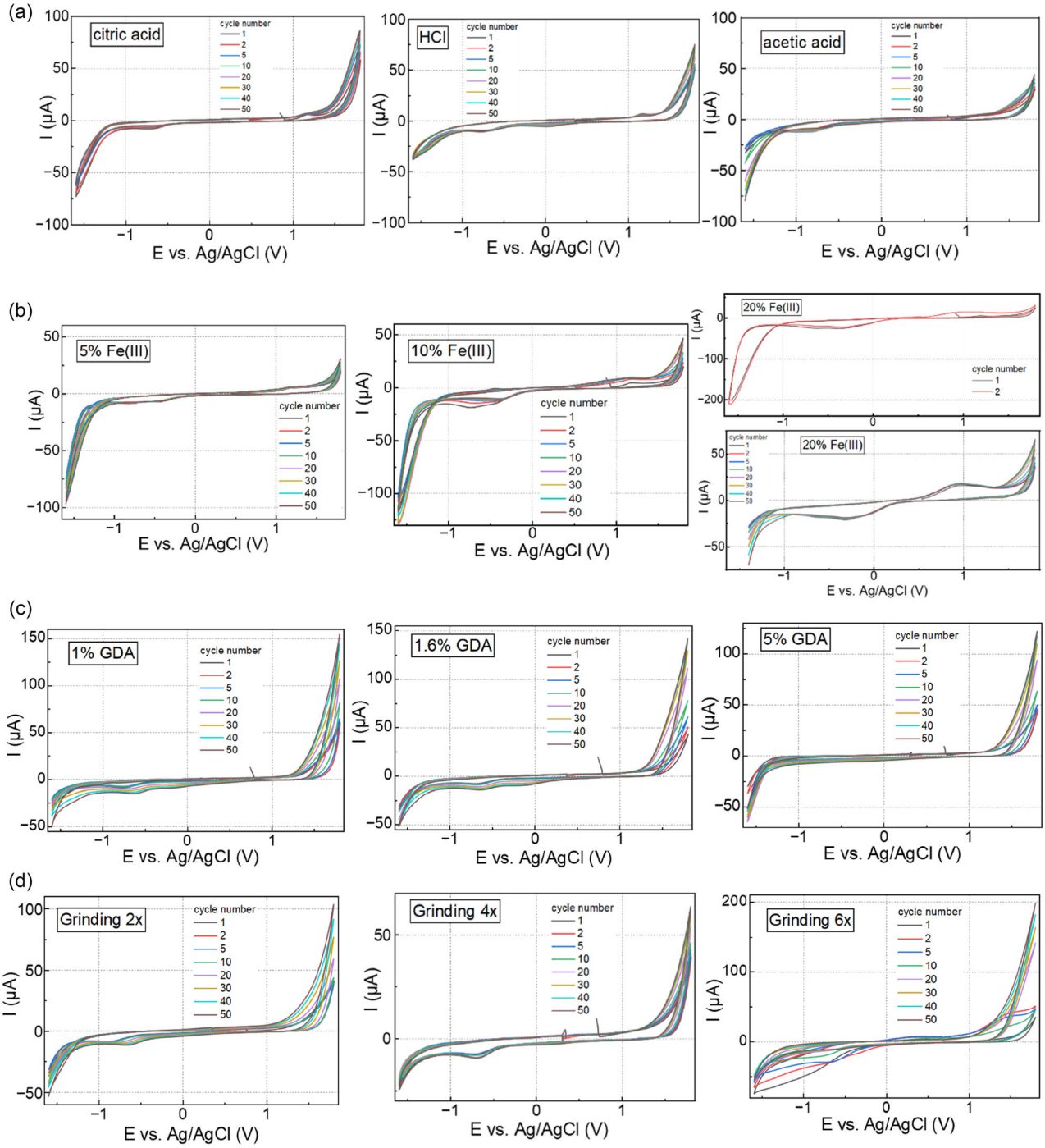

FIGURE 3 | Studies of the electrochemical stability window for collagen dispersions with pH = 3 in dependence on different modifications: (a) impact of the acid type, (b) influence of the added Fe(III) salt (two potential ranges), (c) influence of the added glutaraldehyde (GDA) concentration, and (d) impact of the grinding grade (fourfold grinding being the standard procedure).

acid and hydrochloric acid (Figure 4a). Hydrogen evolution and/or reduction of the carboxyl groups of acetic/citric acids can be the reason for the increase of the current in cyclic voltammograms close to 0 V versus Zn. The reduction is quasi reversible: a broad oxidation peak between 0.5 V and 1.0 V is visible for acetic acid, while shifted to 0.8–1.2 V for citric acid. These processes are not visible in the case of the HCl containing dispersion. The influence of Fe(III) cations by chelate bonding with carboxyl and amino groups on collagen redox activity showed increasing redox activity with increasing Fe amount. An increased grinding grade of the collagen dispersion leads to a higher part of pseudocapacitive contribution due to reduced particle size.

3.4 | Electrochemical Tests of Zn Batteries with $Na_3V_2(PO_4)_3$, $Na_{0.44}MnO_2$ and V_2O_5-PEDOT Cathodes and Collagen Binders

Zinc battery cells with a NVP cathode were galvanostatically tested with collagen dispersions with pH = 3 and pH = 7 and

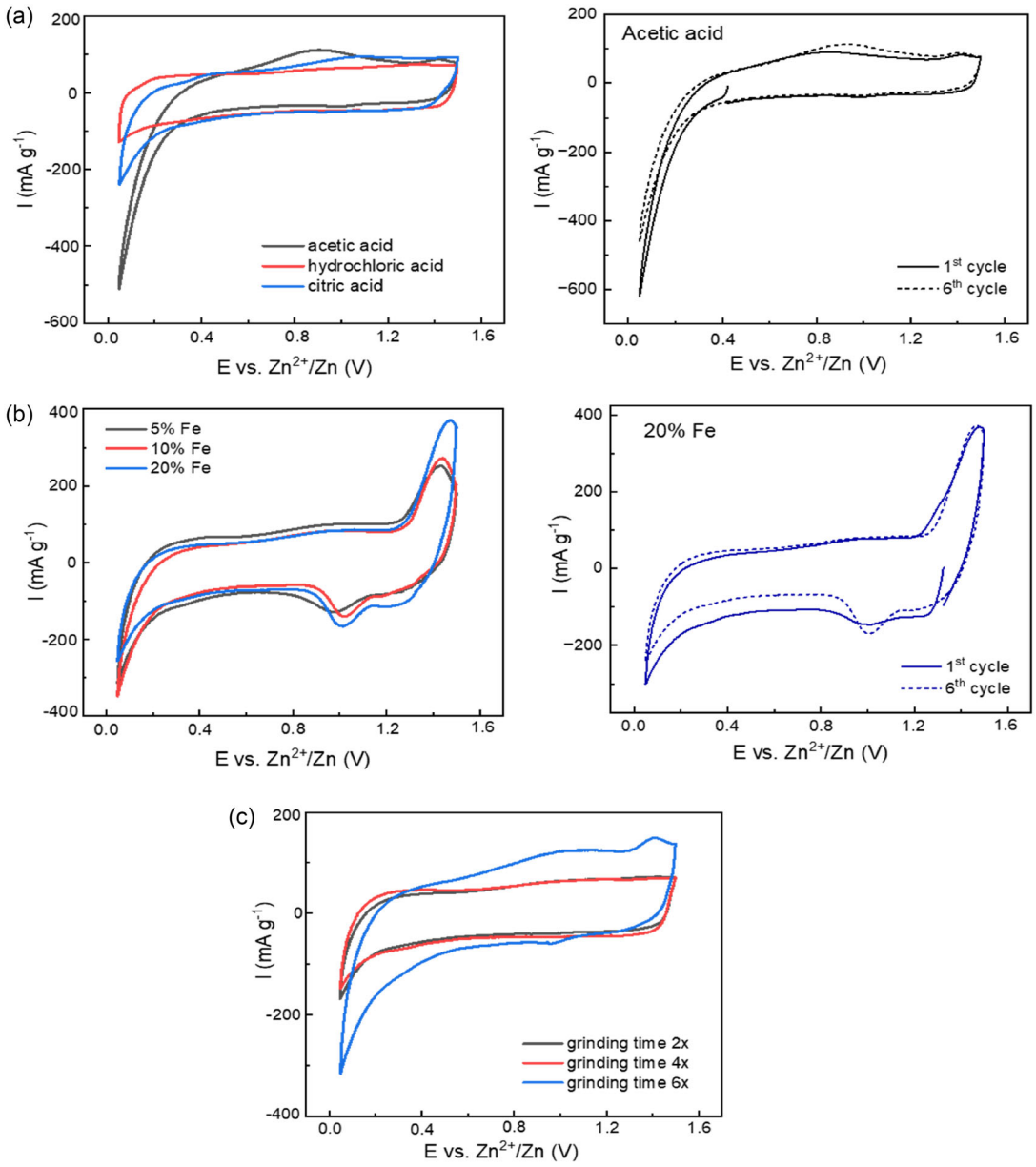

FIGURE 4 | Electrochemical behavior of collagen dispersions as electrode in aqueous Zn cells with a 3 M Zn triflate electrolyte solution. Impact of various modifications of collagen was evaluated: (a) acid type, (b) Fe(III) salt concentration, and (c) grinding grade.

1% dry mass content as a binder (Figure 5). As a reference, NVP electrode with PVDF binder was subjected to the same operating procedure. No additional protection was applied to the Zn metal anode.

From the literature, it is known that NVP material decomposes irreversibly in Zn batteries into $Zn_3V_2O_8$, VO_2, and V_2O_5 during charging (oxidation) [50], what leads to a capacity decay and decreasing average working potential of the cell. Low current rates should additionally support this decomposition. Mild acidic electrolytes facilitate capacity loss in comparison to a neutral electrolyte solution due to a partial vanadium dissolution [50]. There are some measures to maintain the battery capacity like protective surface coating on the NVP material [50, 51], or electrolyte design [50, 52]. Coating provides a mechanical barrier around NVP particles and can prevent dissolution of vanadium species, still enabling the change of the reaction mechanism with decomposition of $Na_3V_2(PO_4)_3$. In contrast, electrolyte modification via adding Na cations to the Zn electrolyte solution prevents the destruction of the $Na_3V_2(PO_4)_3$ structure. In this case, Na insertion/removal into/from the structure represents the main reaction process. The role of the binder for the change in reaction processes in NVP from high-capacity, high-voltage behavior to low-capacity and low-voltage behavior was not studied until now.

Typical electrochemical behavior of battery cells with collagen of different pH values and PVDF, operated at a very low current of 14 mA g^{-1}, is shown in Figure 5a–c. According to the literature, the initial capacity of NVP in Zn batteries corresponds to 90 mAh g^{-1} at current densities between 50 and 100 mA g^{-1} [50, 52]. Our cells showed capacities slightly exceeding 100 mAh g^{-1} for the first charge/discharge cycle (Figure 5a,b), probably due to the lower current rate. During the next few cycles, a noticeable capacity decrease to 50–60 mAh g^{-1} occurred in the cells with the acidic

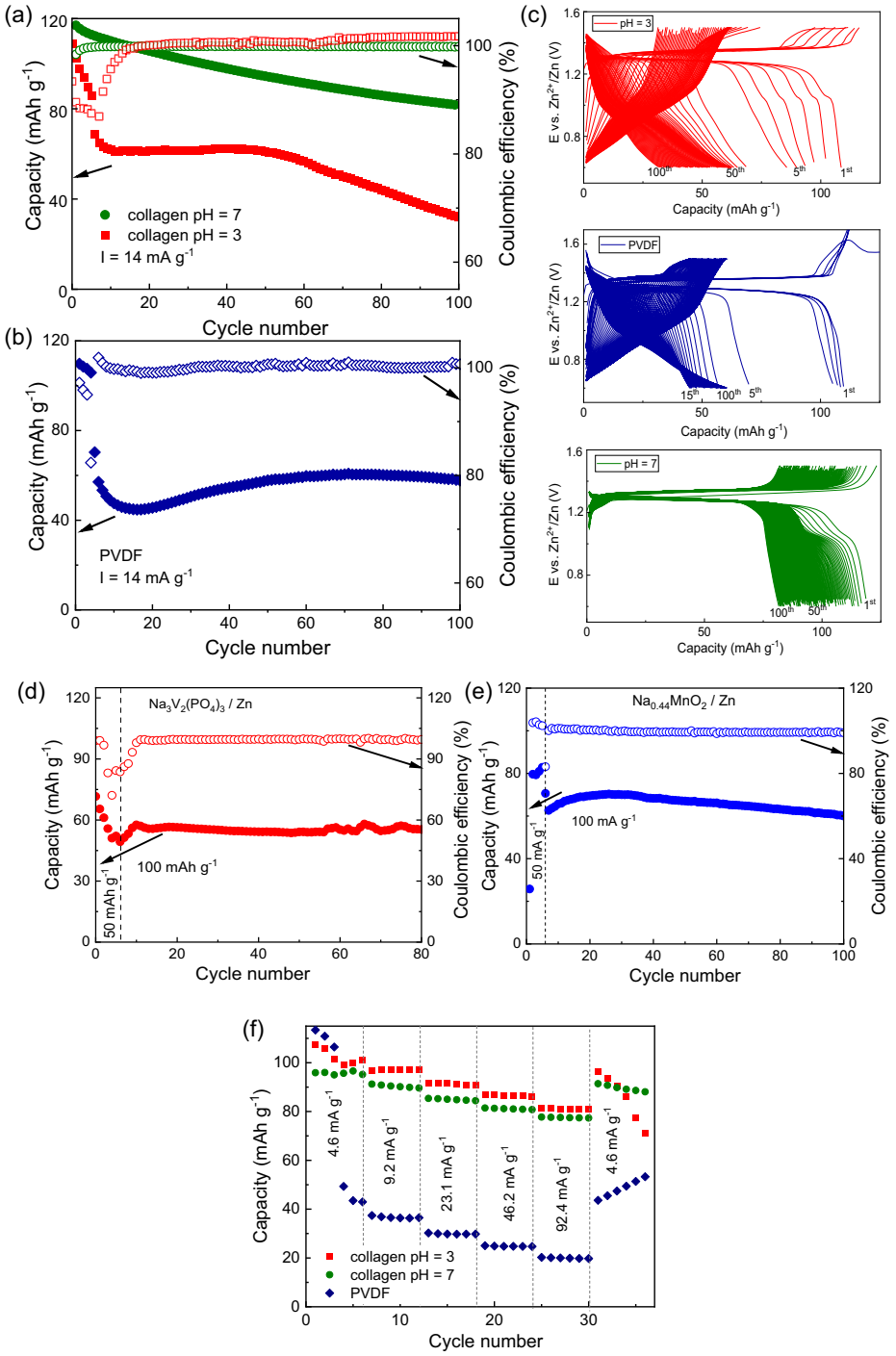

FIGURE 5 | Electrochemical performance of Zn batteries with NVP cathode, containing (a) collagen binder (pH = 3, pH = 7) and (b) PVDF binder, at a current density of 14 mA g^{-1}. (c) Time-dependent electrochemical profile of three cells. Galvanostatic cycling of Zn battery cells with NVP (d) and NMO (e) cathodes and collagen binder (pH = 3) at a current density of 100 mA g^{-1}. The first several cycles were done with 50 mA g^{-1} current density. (f) Rate capability tests of Zn batteries with NVP cathode and binders collagen (pH = 3, pH = 7) and PVDF.

collagen (pH = 3) and PVDF binder, while a much slower capacity decay was observed for the neutral collagen dispersion (pH = 7). Alteration of galvanostatic curves with time (Figure 5c) apparently shows a change in the reaction mechanisms (decomposition of NVP) for the cells with the acidic collagen and PVDF, while preserving the same reaction process for the neutral collagen dispersion. The coulombic efficiency of cells with collagen pH = 3 and PVDF passes through a minimum, reflecting much lower discharging capacity in comparison to the charging one for several cycles, in which the phase transformation occurs. Therefore, the irreversible phase transformation occurs mostly during battery charge, in agreement with the proposed decomposition scheme of NVP [50]. In contrast, the coulombic efficiency of cells with collagen pH = 7 was almost close to 100 % during cycling.

In cells with decomposed NVP and binders PVDF or collagen at pH = 3, the capacity value stabilizes at about 60 mA g^{-1} for the 50^{th} cycle, which is in accordance with the literature reports. However, the cells with the acidic collagen show further

decreasing capacity, which could be attributed to a continuous dissolution of the active material in the electrolyte and removal from the reaction zone [50]. A higher current rate of 100 mA g^{-1} stabilizes to a certain extent the capacity value at 55–60 mAh g^{-1} for a longer time (Figure 5d), probably hindering the dissolution of vanadium.

Rate capability tests of NVP/Zn cells with binders collagen (pH = 3 and pH = 7) and PVDF, and 3 M Zn-triflate electrolyte solution (Figure 5f) with the mass loading varied between 1.61 mg (collagen pH = 3), 5.21 mg (collagen pH = 7) and 5.8 mg (PVDV), showed behavior similar to the observed one for the battery cells subjected to galvanostatic cycling at a low current density. Thus, the cells with collagen binder at pH = 7 showed a stable cycling at all current densities, while the cells with PVDF pointed to a phase transformation with capacity decrease already at the very beginning of charge–discharge treatment. NVP in the cells with collagen at pH = 3 underwent phase transformation at the end of the rate capability test, when a low current density was applied for the second time. NVP with collagen at pH = 7 did not demonstrate any phase transformations during the entire rate capability test. The cell with PVDF demonstrated increasing capacity at low current after NVP structure decomposition. This effect is probably originating from the high loading with active material (5.8 mg).

Like NVP, the $Na_{0.44}MnO_2$ cathode shows a rather stable behavior with the acidic binder dispersion in Zn batteries (Figure 5e) at a high current rate of 100 mA g^{-1}, providing also capacity values overperforming the literature data [53]. Similar to NVP, acidic environment could support the destruction of the $Na_{0.44}MnO_2$ crystal structure due to a possible disproportion of Mn^{3+} to Mn^{4+} and Mn^{2+} and dissolution of Mn^{2+} in the electrolyte. However, the high current density together with the chelating ability of the collagen functional groups apparently hinders disproportionation of Mn^{3+} and supports integrity of the tunnel-type $Na_{0.44}MnO_2$ structure.

Another cathode material, a V_2O_5-PEDOT composite with collagen or CMC binders, was investigated in Zn batteries at even a higher current density of 1 A g^{-1} (Figure 6). Although V_2O_5 represents a promising cathode material due to its high theoretical specific capacity, it suffers from a poor cyclic stability due to the low electronic conductivity, elemental dissolution, and a low Zn diffusion coefficient [54–57]. These drawbacks can be partially mitigated by using a hybrid inorganic–organic V_2O_5-PEDOT composite, which improves electrochemical kinetics of V_2O_5 and reduces the dissolution of vanadium. According to the literature, the V_2O_5-PEDOT composite can represent various states: (i) V_2O_5 particles coated by PEDOT layers (PEDOT acts as a glue, the V_2O_5 structure is almost preserved), (ii) some PEDOT molecules inserted between V_2O_5 layers (crystallinity is decreased, new reflections appear at smaller 2Theta values in XRD patterns pointing to expansion of the interlayer spaces), and (iii) exfoliated V_2O_5 sheets completely coated by PEDOT, showing low crystallinity. The state of the hybrid composite is strongly influenced by the reaction conditions between V_2O_5 and EDOT components [58] and impacts the electrochemical behavior. Thus, a low initial specific capacity of about 40 mAh g^{-1} was reported in the literature for the V_2O_5-PEDOT composite from a commercial V_2O_5 without inserted PEDOT between the layers. Some activation processes lead to increasing capacity with cycling at 1 A g^{-1} reaching a maximum of 350 $mAhg^{-1}$ after 150 cycles, while nearly a stable capacity of about 400 $mAhg^{-1}$ can be obtained for a composite with the exfoliated structure [58]. Both electrode materials in the cited work were prepared with PVDF binder in N-methylpyrrolidone.

SEM image, XRD pattern, and FTIR spectra (Figure S3) confirm the composite formation with the PEDOT coating layer, retaining the structure of V_2O_5, along with a microsized particle morphology. Using collagen binder for the V_2O_5-PEDOT composite provides small capacity fade upon stable long-term cycling behavior within the voltage window between 1.6 and 0.2 V versus Zn^{2+}/Zn at a current density of 1 A g^{-1} (Figure 6). Note that the cells with collagen pH = 3 reproducibly show a more stable cyclability than with collagen pH = 7 and CMC binders. The latter demonstrate a sudden increase of the charging capacity and a subsequent decrease of the coulombic efficiency, pointing to a secondary redox process around 1.4–1.5 V vs. Zn^{2+}/Zn (Figure S4). A dissolution of vanadium species as a possible reason would lead to a continuous capacity decay, which was not detected and could therefore be ruled out. Starting redox decomposition process of PEDOT above 1.5 V versus Zn^{2+}/Zn can probably be a reason for the observed phenomenon [59], which is suppressed if collagen with pH = 3 is used.

Collagen with pH = 3 was tested as a binder in symmetric double-layer supercapacitors using commercial YP50F carbon as electrode material (Figures S5 and 7). Cyclic voltammetry measurements were carried out between 2 and 500 mV s^{-1} scan rates in the voltage range of 0–0.8 V using Zn and Na triflates and Na_2SO_4 as electrolyte solutions (Figure 7a).

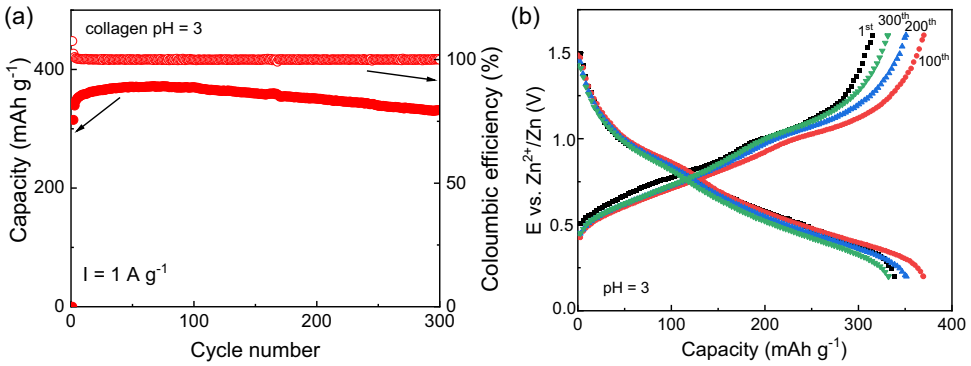

FIGURE 6 | (a) Cycling performance of Zn battery cells with a V_2O_5-PEDOT composite cathode and the collagen binder at pH = 3 and (b) corresponding charge/discharge curves for selected cycles.

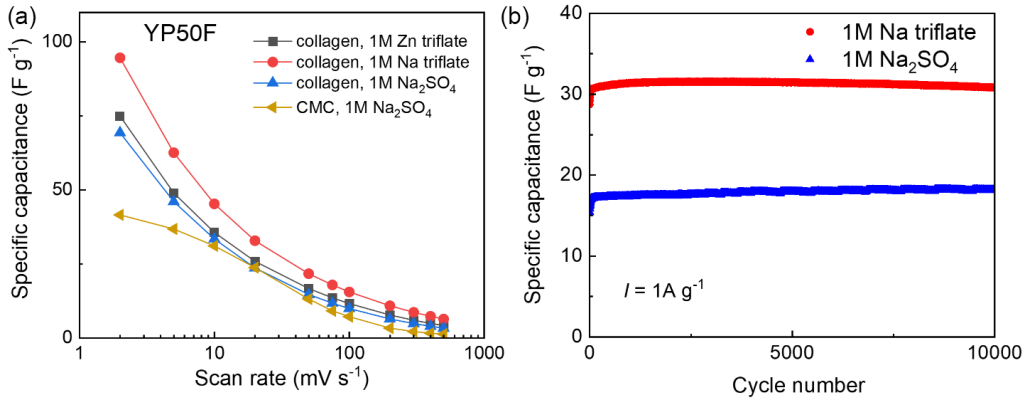

FIGURE 7 | Specific capacitance of the YP50F carbon electrode in symmetric double-layer capacitors in various aqueous electrolyte solutions. As binders, collagen with pH = 3 and CMC were used. (a) calculated from CV measurements at different scan rates and (b) calculated from GCPL measurements at 1 A g^{-1} current density. Voltage range in both types of measurement was 0–0.8 V.

Although room-temperature conductivities of 1 M solutions of Zn and Na triflates lie between 40 and 45 mS cm^{-1} [60], while 66 mS cm^{-1} for 1 M Na_2SO_4 [61], the observed capacities of carbon with collagen binder do not directly correlate with the conductivity values of the electrolytes. The highest specific capacitance at low and intermediate scan rates was observed for monovalent ions (1M Na triflate) followed by divalent ions. The specific capacitance of YP50F with the CMC binder lies below cells with collagen binder, especially at low scan rates. Long-term galvanostatic charge–discharge cycling of symmetric supercapacitors with YP50F carbon performed at a current density of 1 A g^{-1} showed a stable cycling for at least 10 000 cycles, with a higher specific electrode capacitance for 1 M Na triflate electrolyte solution as well (Figure 7b).

4 | Discussion

Due to their electrochemical stability in a broad potential window, tunable viscosity, and cross-linking, ability to swell as well as highly hydrophilic nature together with high availability, collagens represent promising ecological binder systems for aqueous batteries. As a spin-off product of the meat industry, collagen is cheap, easy to produce, and does not contribute to additional environment pollution upon battery utilization/recycling.

High affinity of collagen functional groups to metal cations highlights collagen applicability among other binder systems for aqueous batteries. Carboxyl and particularly amino groups, which are abundant in proteins, are the primary binding sites to metal cations [62, 63]. The bonding ability increases with increasing net negative charge of the protein [64], especially in case of multivalent transition metal cations like Zn, Cr, or Fe, which are known for their stable chelate complexes with collagen functional groups [62, 65, 66]. Therefore, the chelating effect should be more pronounced for neutral and slightly basic collagen dispersions than for the acidic ones, and protonation features an additional degree of freedom upon using collagen as binder. On the other hand, proteins are subjected to hydrolysis in alkaline medium. For this reason, acidic collagen preparations are usually preferred.

In aqueous batteries, both the chelating effect of functional groups and swelling ability of collagen play a big role for the electrochemical performance. Its swelling ability is higher in the acidic environment than in the neutral one due to the positive protein net charge away from the isoelectric point [29]. Therefore, a better covering of particles and closer contact to the current collector are expected when using acidic collagen dispersions. In contrast, collagen at pH = 7 covers particles of the active material less uniformly than at pH = 3.

In aqueous Zn batteries with the $Na_3V_2(PO_4)_3$ cathode, using collagen dispersion with pH = 7 results in an increased concentration of Zn cations around $Na_3V_2(PO_4)_3$ grains due to the complexation of Zn with the functional groups. In the acidic collagen dispersion, positively charged protonated amino groups keep away Zn cations from the cathode due to electrostatic repulsion, leading to less crosslinking. Upon battery cycling, a low current density should in general promote structural degradation of the $Na_3V_2(PO_4)_3$ material. The structural degradation was observed for the cells with PVDF binder and acidic collagen dispersion, while the $Na_3V_2(PO_4)_3$ structure was maintained in the cells with the collagen binder with pH = 7. Therefore, a conventional cation insertion/removal mechanism took place. An open question remains which cations, Zn^{2+}, Na^+, or their mixture, were reversibly inserted/extracted into/from the $Na_3V_2(PO_4)_3$ host, needing more detailed studies in the future. The cells with the acidic collagen showed a continuous capacity decay after structural transformation of the $Na_3V_2(PO_4)_3$ host. Certainly, a higher concentration of protons near to the active material with vanadium ions here accelerates further materials degradation due to the formation of soluble vanadyl-ions.

Increasing current rate during cycling changes the situation significantly. At high current densities, dissolution of vanadium cations seems to be suppressed, and battery cells with vanadium-containing cathode materials can be cycled more stable with the acidic collagen dispersion, as observed for the $Na_3V_2(PO_4)_3$ and V_2O_5-PEDOT composite cathodes. Well-swollen collagen binder at pH = 3 probably also protects PEDOT against onset oxidation [59] at the end of the battery charge. In contrary, long-term cycling behavior of the V_2O_5-PEDOT cathode with collagen pH = 7 or CMC binder irregularly features endless charging curves, reflecting oxidation of the electroactive PEDOT. A lower covering degree of the active material with collagen and CMC cannot stabilize V_2O_5-PEDOT against oxidation. High current densities seem to attenuate the chelating effect of nonprotonated

functional groups of collagens as well. As a conclusion, at high current densities up to 1 A g^{-1}, we observed a repeatable, significantly more stable cycling behavior of the V_2O_5-PEDOT composite cathode with the acidic collagen dispersion than with the CMC binder or neutral collagen.

The electrochemical stability window of the aqueous collagen dispersions lies within the potential window between −1.0 and 1.2 V versus Ag/AgCl reference electrode and is limited rather by water decomposition into H_2 and O_2 than particular instability of collagen.

Further studies on collagen as binder systems for various battery chemistries are necessary, especially a systematic property comparison of modified and non-modified collagens.

5 | Conclusion

We demonstrated the applicability of natural collagen dispersions as binders in aqueous rechargeable Zn batteries and symmetric double-layer supercapacitors. The electrochemical stability window of collagen dispersions without electrolyte salt (2.2 V) is broader than the stability window of conventional aqueous electrolyte solutions (1.5–2.0 V). The pH value of the collagen dispersion certainly influences (electro)chemical processes at the interface between particles of the active material and the electrolyte and can, therefore, partially impact the redox reaction mechanism as we observed for the $Na_3V_2(PO_4)_3$ cathode in Zn batteries with 3 M Zn triflate electrolyte solution.

Nearly a stable cycling behavior of a Zn battery with the V_2O_5-PEDOT composite cathode and collagen binder with pH = 3 was achieved delivering the capacity of 335 mAh g^{-1} for the 300th cycle, which was very close to the initial one. In contrast, neutral collagen dispersion and CMC binder demonstrated less stable behavior due to the onset of PEDOT oxidation.

We also elaborated several possibilities to easily modify rheological properties of collagen dispersions without hampering its electrochemical stability. Among them, grinding grade and cross-linking with glutaraldehyde are the most promising measures to increase the viscosity of the dispersion without increasing the collagen concentration.

Acknowledgments

This work was supported by the Federal Ministry for Economic Affairs and Energy (BMWE) in frame of the research program for the Industrial Collective Research under the project "KoBiNa" (F22685N).

Open Access funding enabled and organized by Projekt DEAL.

Funding

This study was supported by the Federal Ministry for Economic Affairs and Energy (BMWE) (F22685N).

Conflicts of Interest

The authors declare no conflicts of interest.

Data Availability Statement

The data that support the findings of this study are available on request from the corresponding author. The data are not publicly available due to privacy or ethical restrictions.

References

1. H. Chen, M. Ling, L. Hencz, et al., "Exploring Chemical, Mechanical, and Electrical Functionalities of Binders for Advanced Energy-Storage Devices," *Chemical Reviews* 118, no. 18 (2018): 8936–8982, https://doi.org/10.1021/acs.chemrev.8b00241.

2. L. Lu, X. Han, J. Li, J. Hua, and M. Ouyang, "A Review on the Key Issues for Lithium-Ion Battery Management in Electric Vehicles," *Journal of Power Sources* 226 (2013): 272–288, https://doi.org/10.1016/j.jpowsour.2012.10.060.

3. D. Bresser, D. Buchholz, A. Moretti, A. Varzi, and S. Passerini, "Alternative Binders for Sustainable Electrochemical Energy Storage – the Transition to Aqueous Electrode Processing and Bio-Derived Polymers," *Energy and Environmental Science* 11, no. 11 (2018): 3096–3127, https://doi.org/10.1039/c8ee00640g.

4. D. Versaci, R. Nasi, U. Zubair, et al., "New Eco-Friendly Low-Cost Binders for Li-Ion Anodes," *Journal of Solid State Electrochemistry* 21, no. 12 (2017): 3429–3435, https://doi.org/10.1007/s10008-017-3665-5.

5. Z. Zhang, T. Zeng, Y. Lai, M. Jia, and J. Li, "A Comparative Study of Different Binders and Their Effects on Electrochemical Properties of $LiMn_2O_4$ Cathode in Lithium Ion Batteries," *Journal of Power Sources* 247 (2014): 1–8, https://doi.org/10.1016/j.jpowsour.2013.08.051.

6. S. Komaba, K. Shimomura, N. Yabuuchi, T. Ozeki, H. Yui, and K. Konno, "Study on Polymer Binders for High-Capacity SiO Negative Electrode of Li-Ion Batteries," *Journal of Physical Chemistry C* 115, no. 27 (2011): 13487–13495, https://doi.org/10.1021/jp201691g.

7. N. Cuesta, A. Ramos, I. Cameán, C. Antuña, and A. B. García, "Hydrocolloids as Binders for Graphite Anodes of Lithium-Ion Batteries," *Electrochimica Acta* 155 (2015): 140–147, https://doi.org/10.1016/j.electacta.2014.12.122.

8. F. M. Courtel, S. Niketic, D. Duguay, Y. Abu-Lebdeh, and I. J. Davidson, "Water-Soluble Binders for MCMB Carbon Anodes for Lithium-Ion Batteries," *Journal of Power Sources* 196, no. 4 (2011): 2128–2134, https://doi.org/10.1016/j.jpowsour.2010.10.025.

9. V. Dall'Asta, D. Buchholz, L. G. Chagas, et al., "Aqueous Processing of $Na_{0.44}MnO_2$ Cathode Material for the Development of Greener Na-Ion Batteries," *ACS Applied Materials and Interfaces* 9, no. 40 (2017): 34891–34899, https://doi.org/10.1021/acsami.7b09464.

10. P. R. Kumar, Y. H. Jung, S. A. Ahad, and D. K. Kim, "A High Rate and Stable Electrode Consisting of a $Na_3V_2O_2X(PO_4)2F_{3-2X}$–rGO Composite with a Cellulose Binder for Sodium-Ion Batteries," *RSC Advances* 7, no. 35 (2017): 21820–21826, https://doi.org/10.1039/c7ra01047h.

11. J. Zhao, X. Yang, Y. Yao, et al., "Moving to Aqueous Binder: A Valid Approach to Achieving High-Rate Capability and Long-Term Durability for Sodium-Ion Battery," *Advanced Science* 5, no. 4 (2018): 1700768, https://doi.org/10.1002/advs.201700768.

12. M. Gaberscek, M. Bele, J. Drofenik, R. Dominko, and S. Pejovnik, "Improved Carbon Anode for Lithium Batteries - Pretreatment of Carbon Particles in a Polyelectroyte Solution," *Electrochemical and Solid State Letters* 3 (2000): 3.

13. J. Drofenik, M. Gaberscek, R. Dominko, M. Bele, and S. Pejovnik, "Carbon Anodes Prepared from Graphite Particles Pretreated in a Gelatine Solution," *Journal of Power Sources* 94 (2001): 5.

14. R. Dominko, M. Gaberscek, M. Bele, et al., "Understanding the Role of Gelatin as a Pretreating Agent for Use in Li-Ion Batteries," *Journal of the Electrochemical Society* 151 (2004): 5, https://doi.org/10.1149/1.1758813.

15. M. Bele, M. Gaberscek, R. Dominko, et al., "Gelatin-Pretreated Carbon Particles for Potential use in Lithium Ion Batteries," *Carbon* 40 (2002): 6.

16. W. Friess and M. Schlapp, "Effects of Processing Conditions on the Rheological Behavior of Collagen Dispersions," *European Journal of Pharmaceutics and Biopharmaceutics* 51 (2001): 7.

17. A. M. Oechsle, M. Landenberger, M. Gibis, S. B. Irmscher, R. Kohlus, and J. Weiss, "Modulation of Collagen by Addition of Hofmeister Salts," *International Journal of Biological Macromolecules* 79 (2015): 518–526, https://doi.org/10.1016/j.ijbiomac.2015.05.023.

18. A. M. Oechsle, X. Wittmann, M. Gibis, R. Kohlus, and J. Weiss, "Collagen Entanglement Influenced by the Addition of Acids," *European Polymer Journal* 58 (2014): 144–156, https://doi.org/10.1016/j.eurpolymj.2014.06.015.

19. J. Rosenblatt, B. Devereux, and D. G. Wallace, "Injectable Collagen as a pH-Sensitive Hydrogel," *Biomaterials* 15 (1994): 11.

20. K. Gelse, E. Poschl, and T. Aigner, "Collagens—Structure, Function, and Biosynthesis," *Advanced Drug Delivery Reviews* 55, no. 12 (2003): 1531–1546, https://doi.org/10.1016/j.addr.2003.08.002.

21. M. K. Gordon and R. A. Hahn, "Collagens," *Cell and Tissue Research* 339, no. 1 (2010): 247–257, https://doi.org/10.1007/s00441-009-0844-4.

22. K. E. Kadler, C. Baldock, J. Bella, and R. P. Boot-Handford, "Collagens at a Glance," *Journal of Cell Science* 120, no. 12 (2007): 1955–1958, https://doi.org/10.1242/jcs.03453.

23. P. Fratzl, *Collagen - Structure and Mechanics* (Springer, 2008).

24. L. Bozec, G. van der Heijden, and M. Horton, "Collagen Fibrils: Nanoscale Ropes," *Biophysical Journal* 92, no. 1 (2007): 70–75, https://doi.org/10.1529/biophysj.106.085704.

25. B. Brodsky and A. V. Persikov, "Molecular Structure of the Collagen Triple Helix," *Advances in Protein Chemistry* 70 (2005): 39, https://doi.org/10.1016/S0065-3233(04)70009-1.

26. L. M. Delgado, Y. Bayon, A. Pandit, and D. I. Zeugolis, "To Cross-Link or Not to Cross-Link? Cross-Linking Associated Foreign Body Response of Collagen-Based Devices," *Tissue Engineering Part B: Reviews* 21, no. 3 (2015): 298–313, https://doi.org/10.1089/ten.TEB.2014.0290.

27. R. Usha and T. Ramasami, "Structure and Conformation of Intramolecularly Cross-Linked Collagen," *Colloids and Surfaces B: Biointerfaces* 41, no. 1 (2005): 21–24, https://doi.org/10.1016/j.colsurfb.2004.11.001.

28. L. Yang, K. O. van der Werf, P. J. Dijkstra, J. Feijen, and M. L. Bennink, "Micromechanical Analysis of Native and Cross-Linked Collagen Type I Fibrils Supports the Existence of Microfibrils," *Journal of the Mechanical Behavior of Biomedical Materials* 6 (2012): 148–158, https://doi.org/10.1016/j.jmbbm.2011.11.008.

29. M. Meyer, "Processing of Collagen Based Biomaterials and the Resulting Materials Properties," *Biomedical Engineering Online* 18, no. 1 (2019): 24, https://doi.org/10.1186/s12938-019-0647-0.

30. K. Adamiak and A. Sionkowska, "Current Methods of Collagen Cross-linking: Review," *International Journal of Biological Macromolecules* 161 (2020): 550–560, https://doi.org/10.1016/j.ijbiomac.2020.06.075.

31. L. H. H. Olde Damink, P. J. Dijkstra, M. J. A. Van Luyn, P. B. Van Wachem, P. Nieuwenhuis, and J. Feijen, "Glutaraldehyde as a Crosslinking Agent for Collagen-Based Biomaterials," *Journal of Materials Science: Materials in Medicine* 6 (1995): 13.

32. L. H. H. Olde Damink, P. J. Dijkstra, M. J. A. Van Luyn, P. B. Van Wachem, P. Nieuwenhuis, and J. Feijen, "Cross-Linking of Dermal Sheep Collagen Using a Water-Soluble Carbodiimide," *Biomaterials* 17 (1996): 9.

33. N. N. Fathima, B. Madhan, J. R. Rao, B. U. Nair, and T. Ramasami, "Interaction of Aldehydes with Collagen: Effect on Thermal, Enzymatic and Conformational Stability," *International Journal of Biological Macromolecules* 34, no. 4 (2004): 241–247, https://doi.org/10.1016/j.ijbiomac.2004.05.004.

34. M. Jafari-Sabet, H. Nasiri, and R. Ataee, "The Effect of Cross-Linking Agents and Collagen Concentrations on Properties of Collagen Scaffolds," *Journal of Archives in Military Medicine* 4, no. 4 (2016), https://doi.org/10.5812/jamm.42367.

35. L. M. Delgado, K. Fuller, and D. I. Zeugolis, "Collagen Cross-Linking: Biophysical, Biochemical, and Biological Response Analysis," *Tissue Engineering Part A* 23, no. 19-20 (2017): 1064–1077, https://doi.org/10.1089/ten.TEA.2016.0415.

36. T. Covington, *Tanning Chemistry - The Science of Leather* (RSC Publishing, 2009).

37. C. Gaidau, F. Platon, and N. Badea, "Investigation into Iron Tannage," *Journal of the Society of Leather Technologists and Chemists* 82 (1998): 4.

38. Z. Ruszczak and W. Friess, "Collagen as a Carrier for on-Site Delivery of Antibacterial Drugs," *Advanced Drug Delivery Reviews* 55, no. 12 (2003): 1679–1698, https://doi.org/10.1016/j.addr.2003.08.007.

39. J. F. Cavallaro, P. D. Kemp, and K. H. Kraus, "Collagen Fabrics as Biomaterials," *Biotechnology and Bioengineering* 43 (1994): 11.

40. A. J. Bailey, "Collagen - Nature's Framework in the Medical, Food and Leather Industries," *Journal of the Society of Leather Technologists and Chemists* 76.

41. C. H. Lee, A. Singla, and Y. Lee, "Biomedical Applications of Collagen," *International Journal of Pharamceutics* 221 (2001): 23.

42. M. G. Patino, M. E. Neiders, S. Andreana, B. Noble, and R. E. Cohen, "Collagen as an Implantable Material in Medicine and Dentistry," *Journal of Oral Implantology* 28 (2002): 6.

43. W. Li, C. Chen, X. Luo, et al., "Preliminarily Revealing Rheological Behaviors of Mesoscale Collagen Fibrils in Suspension," *Journal of Molecular Structure* 1311 (2024): 138723, https://doi.org/10.1016/j.molstruc.2024.138723.

44. S. Lin, X. Hu, L. Li, et al., "Purification and Identification of Iron-Chelating Peptides Derived from Tilapia (Oreochromis Niloticus) Skin Collagen and Characterization of the Peptide-Iron Complexes," *LWT* 149 (2021), https://doi.org/10.1016/j.lwt.2021.111796.

45. C. Y. Huang, C. H. Wu, J. I. Yang, Y. H. Li, and J. M. Kuo, "Evaluation of Iron-Binding Activity of Collagen Peptides Prepared from the Scales of Four Cultivated Fishes in Taiwan," *Journal of Food and Drug Analysis* 23, no. 4 (2015): 671–678, https://doi.org/10.1016/j.jfda.2014.06.009.

46. S. Ber, G. Torun Kose, and V. Hasirci, "Bone Tissue Engineering on Patterned Collagen Films: An In Vitro Study," *Biomaterials* 26, no. 14 (2005): 1977–1986, https://doi.org/10.1016/j.biomaterials.2004.07.007.

47. N. Dagalakis, J. Flink, P. Stasikelis, J. F. Burke, and I. V. Yannas, "Design of an Artificial Skin. Part III. Control of Pore Structure," *Journal of Biomedical Materials Research* 14, no. 4 (1980): 511–528, https://doi.org/10.1002/jbm.820140417.

48. A. Weber, N. Keim, P. Koch, M. Muller, W. Bauer, and H. Ehrenberg, "The Impact of Binder Polarity on the Properties of Aqueously Processed Positive and Negative Electrodes for Lithium-Ion Batteries," *Scientific Reports* 15, no. 1 (2025): 10024, https://doi.org/10.1038/s41598-025-93813-9.

49. F. Gartner, B. Sundararaju, A. E. Surkus, et al., "Light-Driven Hydrogen Generation: Efficient Iron-Based Water Reduction Catalysts," *Angewandte Chemie International Edition* 48, no. 52 (2009): 9962–9965, https://doi.org/10.1002/anie.200905115.

50. W. Li, X. Jing, K. Jiang, and D. Wang, "Observation of Structural Decomposition of $Na_3V_2(PO_4)_3$ and $Na_3V_2(PO_4)_2F_3$ as Cathodes for Aqueous Zn-Ion Batteries," *ACS Applied Energy Materials* 4, no. 3 (2021): 2797–2807, https://doi.org/10.1021/acsaem.1c00067.

51. B. Tekin, "Nafion-Protected $Na_3V_2(PO)_4)_3$ Electrodes for Aqueous Zinc-Ion Batteries: A Breakthrough in Dissolution Resistance and

Electrochemical Enhancement," *Materials Science and Engineering: B* 307 (2024): 117534, https://doi.org/10.1016/j.mseb.2024.117534.

52. G. Guo, X. Tan, K. Wang, and H. Zhang, "High-Efficiency and Stable Zn−$Na_3V_2(PO_4)_3$ Aqueous Battery Enabled by Electrolyte-Induced Interphasial Engineering," *ChemSusChem* 15, no. 11 (2022): e202200313, https://doi.org/10.1002/cssc.202200313.

53. X. Zhou, A. Zhao, Z. Chen, and Y. Cao, "Research Progress of Tunnel-Structural $Na0.44MnO_2$ Cathode for Sodium-Ion Batteries: A Mini Review," *Electrochemistry Communications* 122 (2021), https://doi.org/10.1016/j.elecom.2020.106897.

54. Y. Dong, M. Jia, Y. Wang, et al., "Long-Life Zinc/Vanadium Pentoxide Battery Enabled by a Concentrated Aqueous $ZnSO_4$ Electrolyte with Proton and Zinc Ion Co-Intercalation," *ACS Applied Energy Materials* 3, no. 11 (2020): 11183–11192, https://doi.org/10.1021/acsaem.0c02126.

55. N. Zhang, M. Jia, Y. Dong, et al., "Hydrated Layered Vanadium Oxide as a Highly Reversible Cathode for Rechargeable Aqueous Zinc Batteries," *Advanced Functional Materials* 29, no. 10 (2019), https://doi.org/10.1002/adfm.201807331.

56. N. Zhang, Y. Dong, Y. Wang, et al., "Ultrafast Rechargeable Zinc Battery Based on High-Voltage Graphite Cathode and Stable Nonaqueous Electrolyte," *ACS Applied Materials and Interfaces* 11, no. 36 (2019): 32978–32986, https://doi.org/10.1021/acsami.9b10399.

57. N. Zhang, Y. Dong, M. Jia, et al., "Rechargeable Aqueous Zn–V_2O_5 Battery with High Energy Density and Long Cycle Life," *ACS Energy Letters* 3, no. 6 (2018): 1366–1372, https://doi.org/10.1021/acsenergylett.8b00565.

58. Y. Liu, T. Wang, Y. Sun, et al., "Fast and Efficient in-Situ Construction of Low Crystalline PEDOT-Intercalated V_2O_5 Nanosheets for High-Performance Zinc-Ion Battery," *Chemical Engineering Journal* 484 (2024): 149501, https://doi.org/10.1016/j.cej.2024.149501.

59. M. Ujvári, M. Takács, S. Vesztergom, F. Bazsó, F. Ujhelyi, and G. G. Láng, "Monitoring of the Electrochemical Degradation of PEDOT Films on Gold Using the Bending Beam Method," *Journal of Solid State Electrochemistry* 15, no. 11-12 (2011): 2341–2349, https://doi.org/10.1007/s10008-011-1472-y.

60. G. R. Pastel, M. S. Ding, T. P. Pollard, O. Borodin, M. Schroeder, and K. Xu, "Cation-Dependent Solvation Behavior of Aqueous Triflate Electrolytes," *ACS Electrochemistry* 1, no. 4 (2025): 486–493, https://doi.org/10.1021/acselectrochem.4c00100.

61. J. Fischer, B. Pohle, E. Dmitrieva, K. Thümmler, S. Fischer, and D. Mikhailova, "Symmetric Supercapacitors with Cellulose-Derived Carbons and Na_2SO_4 Electrolytes Operating in a Wide Temperature Range," *Journal of Energy Storage* 55 (2022), https://doi.org/10.1016/j.est.2022.105725.

62. L. Chen, X. Shen, and G. Xia, "Effect of Molecular Weight of Tilapia (Oreochromis Niloticus) Skin Collagen Peptide Fractions on Zinc-Chelating Capacity and Bioaccessibility of the Zinc-Peptide Fractions Complexes In Vitro Digestion," *Applied Sciences* 10, no. 6 (2020), https://doi.org/10.3390/app10062041.

63. D. Chen, Z. Liu, W. Huang, Y. Zhao, S. Dong, and M. Zeng, "Purification and Characterisation of a Zinc-Binding Peptide from Oyster Protein Hydrolysate," *Journal of Functional Foods* 5, no. 2 (2013): 689–697, https://doi.org/10.1016/j.jff.2013.01.012.

64. M. C. Udechukwu, B. Downey, and C. C. Udenigwe, "Influence of Structural and Surface Properties of Whey-Derived Peptides on Zinc-Chelating Capacity, and In Vitro Gastric Stability and Bioaccessibility of the Zinc-Peptide Complexes," *Food Chemistry* 240 (2018): 1227–1232, https://doi.org/10.1016/j.foodchem.2017.08.063.

65. K. Meng, L. Chen, G. Xia, and X. Shen, "Effects of Zinc Sulfate and Zinc Lactate on the Properties of Tilapia (Oreochromis Niloticus) Skin Collagen Peptide Chelate Zinc," *Food Chemistry* 347 (2021): 129043, https://doi.org/10.1016/j.foodchem.2021.129043.

66. L. Guo, P. A. Harnedy, M. B. O'Keeffe, et al., "Fractionation and Identification of Alaska Pollock Skin Collagen-Derived Mineral Chelating Peptides," *Food Chemistry* 173 (2015): 536–542, https://doi.org/10.1016/j.foodchem.2014.10.055.

Supporting Information

Additional supporting information can be found online in the Supporting Information section.